

# Properties of internal diffusion barrier in high density plasmas on Large Helical Device

Ryuichi SAKAMOTO<sup>1)</sup>, Masahiro KOBAYASHI<sup>1)</sup>, Junichi MIYAZAWA<sup>1)</sup>, Satoshi OHDACHI<sup>1)</sup>, Tomohiro MORISAKI<sup>1)</sup>, Suguru MASUZAKI<sup>1)</sup>, Ichihiro YAMADA<sup>1)</sup>, Motoshi GOTO<sup>1)</sup>, Katsumi IDA<sup>1)</sup>, Shigeru MORITA<sup>1)</sup>, Satoru SAKAKIBARA<sup>1)</sup>, Kenji TANAKA<sup>1)</sup>, Kazuo KAWAHATA<sup>1)</sup>, Kiyomasa WATANABE<sup>1)</sup>, Yasuhiro SUZUKI<sup>1)</sup>, Hisamichi FUNABA<sup>1)</sup>, Sadayoshi MURAKAMI<sup>2)</sup>, Naoko ASHIKAWA<sup>1)</sup>, Yoshio NAGAYAMA<sup>1)</sup>, Yoshiro NARUSHIMA<sup>1)</sup>, Byron J. PETERSON<sup>1)</sup>, Mamoru SHOJI<sup>1)</sup>, Chihiro SUZUKI<sup>1)</sup>, Masayuki TOKITANI<sup>1)</sup>, Shinji YOSHIMURA<sup>1)</sup>, Nobuyoshi OHYABU<sup>1)</sup>, Hiroshi YAMADA<sup>1)</sup>, Akio KOMORI<sup>1)</sup>, Osamu MOTOJIMA<sup>1)</sup> and LHD experimental group<sup>1)</sup>

<sup>1)</sup>National Institute for Fusion Science, Japan

<sup>2)</sup>Kyoto University, Japan

An experimental study is performed in order to extend the operational space of internal diffusion barrier (IDB) plasma, which was originally found in pellet fueled high density discharges with the local island divertor configuration, to an intrinsic helical divertor configuration in large helical device (LHD). It is revealed that the IDB can be reproducibly formed in intrinsic helical divertor configurations as in the local island divertor configuration. The IDB is efficiently formed by central pellet fueling in the outer shifted magnetic configuration ( $R_{ax} > 3.7$  m). Attainable core plasma density becomes higher as the magnetic axis shifts outward. Maximum core density reaches  $1 \times 10^{21} \text{ m}^{-3}$ . Central pressure exceeds 130 kPa, and therefore very large Shafranov shift ( $\Delta/a_{\text{eff}} \geq 1/2$ ) due to high central beta is observed even at high magnetic field ( $B_t \sim 2.54$  T).

Keywords: stellarator, internal diffusion barrier, pellet fueling, divertor, magnetic configuration

## 1 Introduction

Confinement improvement is one of the most important issues of magnetic confined fusion plasma research. The internal diffusion barrier (IDB) which enables core plasma to access high-density/high-pressure regime has been found in multi pellets fueled high density discharges with an active pumped local island divertor (LID) configuration in large helical device (LHD) [1]. A high density core plasma with  $5 \times 10^{20} \text{ m}^{-3}$  is maintained by the IDB located at  $\rho = 0.5$  and the IDB plasma exhibit the highest fusion triple product on LHD,  $n_0 T_0 \tau_E = 4.4 \times 10^{19} \text{ keV m}^{-3} \text{ s}$ .

The IDB is similar to pellet enhanced performance (PEP) mode, which is first found in JET[2] then in the other tokamaks [3, 4], on the point that both lead to strongly peaked pressure profile. On the other hand, unlike the tokamak PEP mode, there is no clear indication of increase in the temperature gradient and inward particle convection in IDB. Although the LID configuration has efficient pumping due to the localized installation, heat removal is problem for the same reason with the present LID design. Therefore, IDB formation in intrinsic helical divertor configuration which have larger heat receiving area than LID configuration is highly desired from a standpoint of com-

patibility with a fusion reactor.

An experimental study has been performed in order to explore the operational space of the IDB discharge with the intrinsic helical divertor configuration in LHD.

## 2 Experimental Set-up

LHD is a heliotron type full superconducting stellarator with a pair of continuously wound  $M = 10$  helical coils and three pairs of poloidal coils. The plasma major radius at vacuum magnetic field is variable in the range of 3.5 m to 4.0 m, the averaged plasma minor radius is  $\sim 0.6$  m and the magnetic field strength is  $\leq 3$  T[5]. A helical divertor is intrinsic divertor configuration in heliotron type device. The divertor has open structure with forced water-cooled carbon target plate and there is no pumping capacity except wall pumping. The heat receiving area is about 50 times larger than LID configuration and it allow high heating power and long pulse experiments.

Three negative ion based high energy (up to 180 keV) neutral beam injector (NBI) are employed for plasma heating. Typical NBI heating power is 12 MW in total. Solid hydrogen ice pellets are launched from outboard side mid-plane by using 10 barrels *in-situ* pipe-gun pellet injector[6]. The typical pellet mass and velocity are

$1.5 - 2.0 \times 10^{21}$  atoms per pellet and 1000-1200 m/s, respectively.

### 3 Internal Diffusion Barrier Formation in Helical Divertor Configuration

#### 3.1 fueling

Typical plasma profiles of the gas-puff and pellet fueled discharges at the same magnetic configuration  $R_{ax} = 3.75$  m in the same line integrated density  $n_e l = 3 \times 10^{20} \text{ m}^{-2}$  are shown in figure 1. The normalized minor radius  $\rho$  is expressed as flux coordinate, namely,  $\rho = \sqrt{\Phi}$  where  $\Phi$  is the toroidal flux function, which is normalized by the value of the last closed flux surface. The negative and positive  $\rho$  value indicate inboard and outboard side of the plasma, respectively. Since particle source is limited to peripheral for the gas-puff fueling, the density profile typically becomes flat or slightly hollow. In the case of the pellet fueling, the IDB which has a steep density gradient inside  $\rho = 0.55$  is formed and the central density is remarkably increased while peripheral density is reduced. A noteworthy finding is that the electron temperature of the pellet fueled plasma is higher in spite of the fact that the central density is more than double. The plasma pressure profile calculated assuming the ion temperature profile is the same as measured electron temperature profile, show an obvious increase of the plasma energy density in the core region ( $\rho < 0.55$ ).

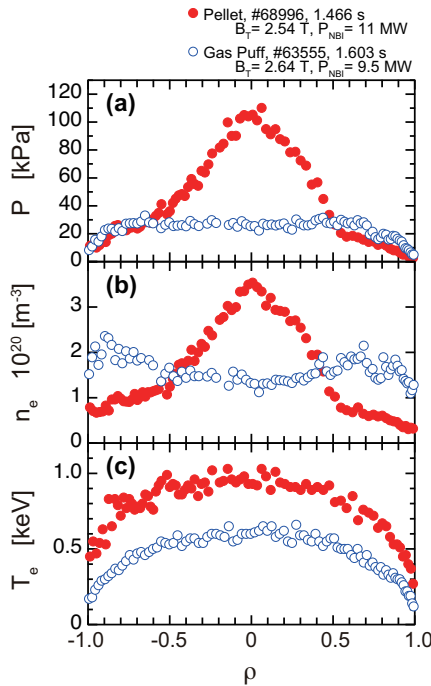


Fig. 1 Comparison of (a) Plasma pressure, (b) electron density and (c) electron temperature in the gas-puff (blue open circle) and pellet (red filled circle) fueled discharges at the same magnetic configuration  $R_{ax} = 3.75$  m.

The attainable central pressure of the pellet fueled plasma is about four times larger than that of the gas-puff fueled plasma, even exceeding atmospheric pressure. The plasma  $\beta$  becomes high even though the magnetic field is high ( $B_t > 2.54$  T) and thus the plasma profiles suffer very large Shafranov shift ( $\Delta/a_{\text{eff}} \sim 1/2$ ).

#### 3.2 pre-set magnetic axis

The global energy confinement time reaches a maximum in inward shifted magnetic configurations ( $R_{ax} = 3.60 - 3.65$  m which give a maximum plasma volume) by employing pellet fueling[7]. The IDB, on the other hand, is easy to produce in outward shifted magnetic configurations ( $R_{ax} > 3.7$  m). One characteristic difference between configurations is magneto-hydrodynamic stability properties, considered to be favorable as the magnetic axis shifts outward[8] because the region with magnetic well is wide, especially at finite  $\beta$ . It is also important that the poloidal distribution of a divertor flux changes with magnetic configurations[9]. The divertor flux tends to concentrate on the inboard side and this leads to a localized increase of neutral pressure due to recycling in the inward shifted magnetic configurations. This situation is estimated to cause a peripheral density rise which is incompatible with the core fueling. Contrary to this, the divertor flux tends to spread uniformly poloidally in the outward shifted magnetic configurations and this behavior leads to suppression of peripheral particle source. This situation is expected to compensate the lack of pumping capacity at helical divertor.

Figure 2 shows the temporal evolution of characteristic plasma parameters in several nine-pellet fueled discharges at magnetic axes  $R_{ax} = 3.65$  m,  $3.75$  m and  $3.85$  m. Let timing of the final pellet injection be  $t = 0$ . In each cases, NB heating power and magnetic strength are 11 MW and 2.54 T, respectively. The IDB formation period is denoted by filled symbol. It is difficult to define onset and termination timing of the IDB regime because the IDB profile gradually changes in time. The IDB is temporarily defined by existence of a clear bend in the density profile. While the same number of pellets were injected, attainable central plasma density becomes higher as the magnetic axis shifts outward and the maximum central density at  $R_{ax} = 3.85$  m is doubled compare to the density at  $R_{ax} = 3.65$  m. At the same time, the central temperature follows quite a similar course after pellet injection although central density varies widely depending on magnetic configuration. As the result, higher central pressure is attainable in the outward shifted magnetic configurations where the IDB is formed. The point to observe is that there is a plateau of the pressure rise in the high density phase as shown by two-headed arrows in figure 2(a). The plateau begins to appear during the pellet injection phase, namely density increase phase, and continues until the excess density drops to the onset level. This phenomenon indicates

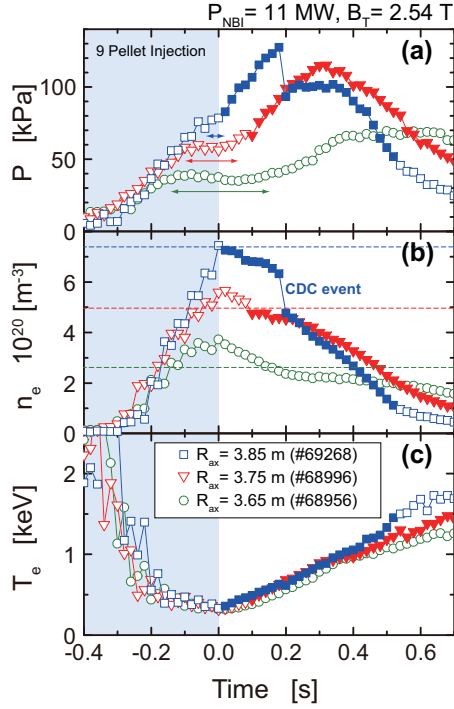


Fig. 2 The temporal evolution of (a) Plasma pressure, (b) electron density and (c) electron temperature in nine-pellets fueled discharges at magnetic axes  $R_{ax} = 3.65$  m (green circle),  $3.75$  m (red triangle) and  $3.85$  m (blue square). The magnetic field strength and NB heating power are  $2.54$  T and  $11$  MW, respectively. Filled symbols denote the formation of IDB.

confinement degradation in high density regime. As the magnetic axis shifts outward, the onset density level increase as indicated by broken line in figure 2(b), namely  $2.7 \times 10^{20} \text{ m}^{-3}$  at  $R_{ax} = 3.65$  m and  $5.0 \times 10^{20} \text{ m}^{-3}$  at  $R_{ax} = 3.75$  m, and duration of the plateau becomes shorter. Finally the plateau of the pressure rise is hardly observed at  $R_{ax} = 3.85$  m and the pressure is increase in a linear fashion during and after pellet injection. After that, the pressure and density decrease suddenly at  $t = 0.18$  s, while any noticeable changes are not observed in the temperature. This unexpected event is referred to as core density collapse (CDC) and will be discussed later. It must be also noted that the final density levels out after the disappearance of the IDB. The final density becomes lower as the magnetic axis shifts outward, contrary to the IDB phase, and this observation supports a reduced recycling in the outward shift configurations.

Figure 3 shows a comparison of plasma profiles between  $R_{ax} = 3.65$  m and  $3.75$  m at the timing of  $T_e(0) = 1$  keV. Density profiles of the two configurations are quite different even though the temperature profiles are identical. For  $R_{ax} = 3.65$  m, the density profile has a parabolic shape. On the other hand, the IDB with steep density gradient is formed on the inside of  $\rho = 0.55$  and central density reached to almost double in the case of  $R_{ax} = 3.75$  m. Thus magnetic configuration is another factor of the IDB

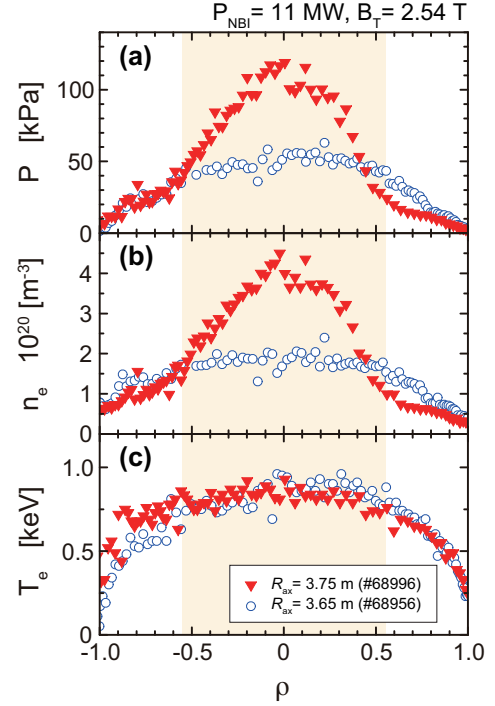


Fig. 3 Comparison of (a) Plasma pressure, (b) electron density and (c) electron temperature between  $R_{ax} = 3.65$  m (blue open circle) and  $3.75$  m (red filled triangle) at the timing of  $T_e(0) = 1$  keV. The magnetic field strength and NB heating power are  $2.54$  T and  $11$  MW, respectively. Hatching denotes IDB formation region.

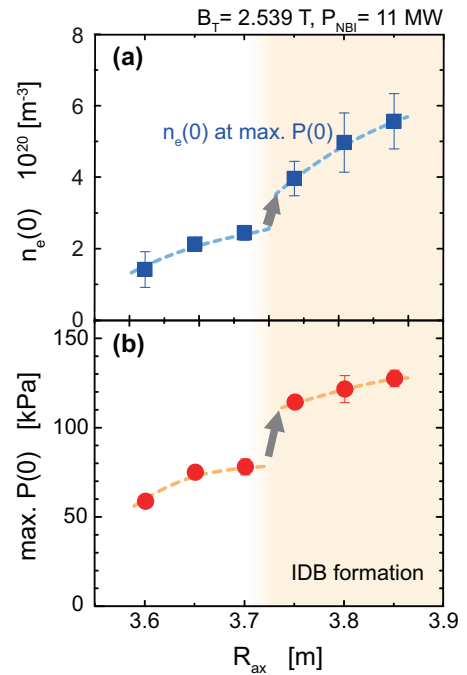


Fig. 4 Configuration dependence of (a) central electron density at the instant of maximum central pressure and (b) maximum central pressure. The magnetic field strength and NB heating power are  $2.54$  T and  $11$  MW, respectively.

formation in addition to pellet core fueling.

The magnetic axis dependence of the IDB plasmas is summarized in figure 4. Attainable central density becomes higher as the magnetic axis shifts outward and the central density exceeds  $5 \times 10^{20} \text{ m}^{-3}$ . The point to observe is that there is a sharp increase in central density and pressure around  $R_{ax} = 3.7 \text{ m}$  and central pressure reach its greatest value,  $\sim 130 \text{ kPa}$ , at the neighborhood of  $R_{ax} = 3.85 \text{ m}$ . The maximum central pressure is limited by the CDC event as shown in figure 2.

## 4 Properties of IDB Plasmas

### 4.1 particle transport

Figure 5 shows a change of IDB profiles from moment to moment. The IDB structure, which has localized sharp density gradient, namely box-like density profile, is observed at 1.2 s. Then density gradient is gradually decreases and spread into core region during density decay and temperature recover phase. Finally the IDB structure changes to linear profile at 1.6 s with keeping central pressure. During the profile change, a collisionality  $\nu_b^*$ , which is normalized by a bounce frequency of banana particles, decrease monotonically in the plateau regime ( $10 \geq \nu_b^* \geq 1$ ). This IDB structure change, from box-like profile to linear profile, is explained by lack of particle source inside IDB for the following particle transport analysis.

The particle transport coefficient of IDB plasma is calculated by using relationship between time evolution and gradient of density profiles after pellet injection. Figure

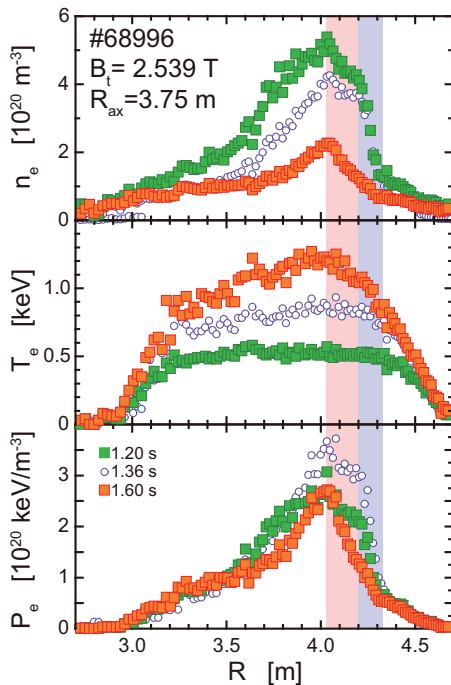


Fig. 5 Change of IDB structure.

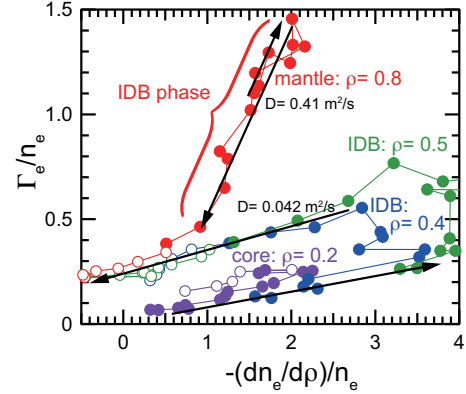


Fig. 6 Particle flux normalized by electron density as a function of density gradient after pellet injection in various minor radius. Filled symbols denote the period of IDB formation.

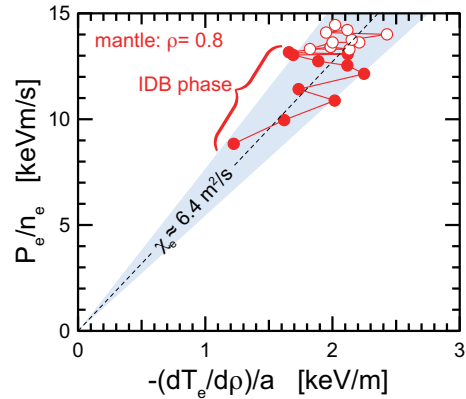


Fig. 7 Heat flux normalized by electron density as a function of temperature gradient after pellet injection in low density mantle ( $\rho = 0.8$ ). Filled symbols denote the period of IDB formation.

6 shows relationship between normalized particle flux and normalized density gradient. Gradient and y-intercept of this plot indicate diffusivity ( $D_e$ ) and convection velocity ( $v_e$ ) according to the following relational expression.

$$\frac{\Gamma_e}{n_e} = -D_e \frac{1}{n_e} \frac{\partial n_e}{\partial \rho} + v_e,$$

where  $\Gamma_e = -\frac{1}{A} \int \frac{\partial n_e}{\partial t} dV$  is particle flux assuming no particle source inside the flux surface. The filled symbols denote the period of IDB formation. Diffusivity of core region inside IDB ( $\rho \geq 0.5$ ) is kept at low level as  $D = 0.042 \text{ m}^2/\text{s}$  even high density gradient and inward convection velocity can not be observed. Therefore IDB core can be described with diffusive nature and the profile change, box-like to linear, is explained by lack of particle source inside IDB. And also the core diffusivity is said to be not sensitive to collisionality in the range of plateau regime. On the other hand, the mantle plasma cannot keep the density gradient in high particle flux IDB phase, namely, mantle diffusivity deteriorates during IDB phase. Notable characteristics of the IDB plasma is that the thermal transport coefficient

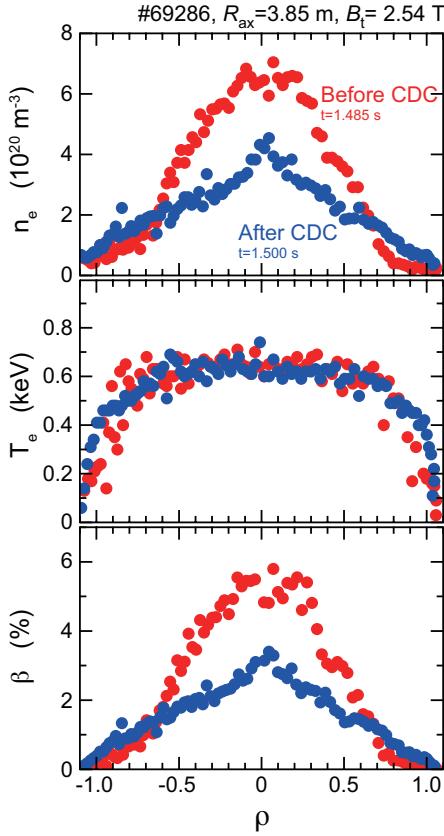


Fig. 8 Change of plasma profiles before and after CDC event.

cient, which is relationship between heat flux and temperature gradient remain unaffected by big change of the particle transport as shown in figure 7. These results lead to separation of confinement region between the IDB core (high density gradient) and low density mantle (high temperature gradient), and therefore high-density/high-pressure plasma is attained in the IDB discharge. The IDB core is formed by the deep pellet fueling and intrinsic good particle confinement property. The low density mantle have advantages to suppress radiation loss, and therefore density limit of IDB plasma is extremely extend to high-density regime. In addition, low density mantle secure temperature gradient for high-density/high-pressure core plasma.

## 4.2 core density collapse event

Figure 8 shows plasma profiles just before and after CDC event. In the CDC event, the high density core plasma is expelled on the sub millisecond time scale () without having any impact on the central temperature. CDC event is typically observed in the high performance discharges with IDB. The mechanism of the CDC is not yet elucidated, but it may be involved with MHD instability and/or equilibrium limit arising from very large Shafranov shift. Therefore, suppression of the Shafranov shift is potential solution to avoid CDC event. Pfirsch-Schlüter current control by a vertical elongation, namely ellipticity  $\kappa$  control, is a means of Shafranov shift suppression [10] in helical sys-

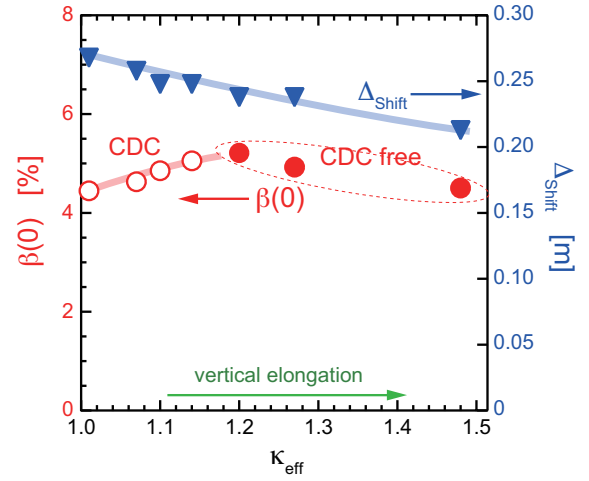


Fig. 9 Shafranov shift amount  $\Delta_{\text{shift}}$  and central beta  $\beta_0$  at the maximum central pressure as a function of the effective ellipticity  $\kappa_{\text{eff}}$ . The filled symbol in  $\beta_0$  denote the occurrence of CDC event.

tem.

Figure 9 shows the Shafranov shift amount and central beta at the maximum central pressure as a function of the effective ellipticity  $\kappa_{\text{eff}}$ , which is defined by ratio of line densities between vertical elongated and horizontally elongated poloidal cross-section. As the  $\kappa_{\text{eff}}$  become large, amount of Shafranov shift monotonically get smaller. Attainable central pressure, which is restricted by CDC event, is become large until  $\kappa_{\text{eff}} = 1.2$  and the attainable central pressure increase by 20 % compare to standard configuration  $\kappa_{\text{eff}} = 1.0$ . Extreme vertical elongation beyond  $\kappa_{\text{eff}} = 1.2$  result in a degradation of central beta although the CDC event is not observed. Under the condition of  $\kappa_{\text{eff}} \geq 1.2$ , MHD instability which is different from CDC event is observed and confinement degradation is suggested.

## 4.3 impurity behavior

In helical system, neoclassical ambipolar diffusion predict ion root (negative radial electric field  $E_r$ ) in high density regime and the negative  $E_r$  lead to impurity accumulation. In general, impurity behavior is one of the most concerned topics in high-density discharges, because radiation collapse due to loss of power balance tends to take place by less impurity contamination than a low density discharges. Contrary to theoretical prediction, significant indication of impurity accumulation is not observed by  $Z_{\text{eff}}$  and bolometric measurements although negative  $E_r$  in the IDB plasma is verified by a charge exchange recombination spectroscopy. Existence of impurity accumulation due to negative radial electric field has not been confirmed, nevertheless impurity contamination is not a significant problem in the IDB discharge. Divertor modeling study using EMC3-EIRENE code suggests impurity shielding po-

tential in ergodic layer [11], namely, outward friction force by plasma flow dominate impurity behavior and impurity tend to be expelled from LCFS in high-density regime.

## 5 Conclusion

An experimental study is performed to explore the operational space of a high density plasmas due to the IDB which was originally found in pellet fueled high density discharges with the active pumped LID configuration in LHD. The IDB with steep density gradient has been produced at an intrinsic helical divertor configuration as in LID configuration by optimizing the pellet fueling and magnetic configuration. Core fueling by multiple pellet injection is essential for the IDB formation and the IDB easily appears in the outer shifted magnetic configuration ( $R_{ax} > 3.7$  m). Confinement region is separated into low density mantle and high density core in IDB plasma. This lead to high-density/high-pressure core plasma. The central density reaches  $1 \times 10^{21} \text{ m}^{-3}$  at  $R_{ax} \geq 3.9$  m and the central pressure has reached 1.3 times atmospheric pressure. Although negative  $E_r$  is verified, harmful impurity contamination has not been observed in IDB plasma. CDC event, which arise from very large Shafranov shift, restrict operational regime. Suppression of Shafranov shift with ellipticity control can mitigate CDC event and the central pressure increase by 20 % of standard configuration. Investigation of long-duration sustainability of the pellet fueled IDB is critically important from a perspective of extrapolation to fusion reactor scenario. Nonetheless, the IDB is an encouraging finding and it demonstrates the potential for alternative path to high-density/low-temperature fusion reactor in helical devices.

This work is supported by NIFS06ULPP521.

- [1] N. Ohya *et al.*, Phys. Rev. Lett. **97**, 055002 (2006).
- [2] JET Team, Plasma Phys. Control. Fusion **30**, 1467 (1988).
- [3] Y. Takase *et al.*, Phys. Plasmas **4**, 1647 (1997).
- [4] L.R. Baylor *et al.*, Phys. Plasmas **7**, 1878 (2000).
- [5] O. Motojima *et al.*, Phys. Plasmas **6**, 1843 (1999).
- [6] H. Yamada *et al.*, Fusion Eng. Des. **49-50**, 915 (2000).
- [7] R. Sakamoto *et al.*, Nucl. Fusion **41**, 381 (2001).
- [8] H. Yamada *et al.*, Plasma Phys. Controlled Fusion **43**, A55 (2001).
- [9] S. Masuzaki *et al.*, Nucl. Fusion **42**, 750 (2001).
- [10] T. Kobuchi *et al.*, Plasma Phys. Controlled Fusion **48**, 789 (2006).
- [11] M. Kobayashi *et al.*, this conference , I-07 (2007).